Nonsequential and Sequential Fragmentation of CO_2^{3+} in Intense Laser Fields

Cong Wu,[1] Chengyin Wu,[1,*] Di Song,[2] Hongmei Su,[2,†] Yudong Yang,[1] Zhifeng Wu,[1] Xianrong Liu,[1] Hong Liu,[1] Min Li,[1] Yongkai Deng,[1] Yunquan Liu,[1] Liang-You Peng,[1] Hongbing Jiang,[1] and Qihuang Gong[1,‡]

[1]*State Key Laboratory for Mesoscopic Physics, Department of Physics, Peking University, Beijing 100871, People's Republic of China*

[2]*State Key Laboratory of Molecular Reaction Dynamics, Beijing National Laboratory for Molecular Sciences, Institute of Chemistry, Chinese Academy of Sciences, Beijing 100190, People's Republic of China*

(Received 10 October 2012; published 7 March 2013)

We experimentally studied the three-body fragmentation dynamics of CO_2 initiated by intense femtosecond laser pulses. Sequential and nonsequential fragmentations were precisely separated and identified for CO_2^{3+} to break up into $O^+ + C^+ + O^+$ ions. With accurate measurements of three-dimensional momentum vectors of the correlated atomic ions and calculations of the high-level *ab initio* potential of CO_2^{3+}, we reconstructed the geometric structure of CO_2^{3+} before fragmentation, which turns out to be very close to that of the neutral CO_2 molecule before laser irradiation. Our study indicated that Coulomb explosion is a promising approach for imaging geometric structures of polyatomic molecules if the fragmentation dynamics can be clearly clarified and the appropriate dissociation potential is provided for multiply charged molecular ions.

DOI: 10.1103/PhysRevLett.110.103601 PACS numbers: 42.50.Hz, 33.80.Rv, 34.50.Gb

Exploration of transient molecular structures is one of the fundamental tasks in physics, chemistry, and biology [1–4]. Femtosecond laser Coulomb explosion imaging has been exhibited to be a feasible approach for monitoring transient molecular structure, in which case the molecule is rapidly ionized by intense femtosecond laser field and the multiply charged molecular ion is quickly fragmented. The molecular structure is then deduced from momentum vectors of correlated fragments [5–7]. However, this method remains challenging for polyatomic molecules because of their complicated fragmentation dynamics. The main question lies in whether the chemical bonds break through a sequential or a nonsequential process. Therefore, fragmentation dynamics must be clarified for multiply charged polyatomic molecular ions before the Coulomb explosion imaging can be used to reconstruct their geometric structures.

As a prototype system of three-body fragmentation, the process of $CO_2^{3+} \rightarrow O^+ + C^+ + O^+$ has been extensively studied with synchrotron radiation [8], fast heavy-ion beams [9], slow highly charged ions [10], as well as intense laser fields with different pulse durations [11–17]. The asymptotic angle O^+:O^+ between the momentum vectors of the two O^+ ions and the kinetic energy release of atomic ions implied that CO_2^{3+} fragments through a nonsequential process in intense femtosecond laser fields. By measuring the momentum vectors of correlated $O^+ + C^+ + O^+$ ions, the geometric structure has been reconstructed for CO_2^{3+} before explosion. Because of the lack of the accurate *ab initio* potential energy surface of CO_2^{3+}, Coulomb potential approximation has always been applied in the reconstruction of transient molecular structures. The results showed that there is a bond stretching and a bent excitation after the laser irradiation [13,16,17]. However, there has been no direct evidence verifying the assumption that the three-body fragmentation of CO_2^{3+} occurs only through the nonsequential process in intense laser fields. This assumption was further questioned after the observation in the collision system between neutral CO_2 molecules and slow highly charged ions, in which CO_2^{3+} was observed to undergo both sequential fragmentation and nonsequential fragmentation [10]. In the case of the sequential fragmentation process, the CO_2^{3+} molecule dissociates into an O^+ ion and a rotating intermediate CO^{2+} ion. Then the rotating intermediate CO^{2+} dissociates into a C^+ ion and a second O^+ ion. The delay between the two O^+ ions ejection is comparable to the rotational period of the intermediate CO^{2+}. In the case of the nonsequential fragmentation process, the two C=O bonds break simultaneously and the atomic ions are driven apart by their Coulomb repulsion. In this Letter, we experimentally studied three-body fragmentation dynamics of CO_2^{3+} in intense femtosecond laser fields. By correlating the kinetic energy of the two O^+ ions, we are able to separate and thus identify unambiguously the nonsequential and sequential fragmentation of CO_2^{3+}. With the high-level *ab initio* potential of CO_2^{3+}, we reconstructed the geometric structure. The bond length is about 1.1 Å for CO_2^{3+} before fragmentation and is very close to that of neutral CO_2 molecules.

In the experiment, we combined a femtosecond laser amplifier and a newly built reaction microscope to study the fragmentation dynamics of CO_2^{3+}. In our reaction microscope [18,19], the supersonic CO_2 molecular beam is diffused into the reaction chamber through a three-stage differential pumping system. The ions and electrons produced in the laser-molecule interaction are accelerated by a uniform electric and magnetic field. Then they fly in opposite directions and, respectively, hit the temporal and position-sensitive detector (RoentDek, Germany). To ensure that all fragmental ions originate from the same target molecule, we controlled the reaction chamber pressure lower than 2×10^{-10} mbar so that there is less than one CO_2 molecule within one pulse in the laser focus. The ionization events were then recorded in the event-by-event list-mode file. In the off-line analysis, we selected the events in which only two O^+ and one C^+ ions are generated in each laser pulse. Also, the momentum sum of the three atomic ions must be less than the initial momentum of the CO_2 molecular beam to ensure real coincidence.

Figure 1(a) shows two-dimensional momentum distributions ($P_\parallel$ and $P_\perp$) in the center-of-mass coordinate frame for the correlated atomic ions $O^+ + C^+ + O^+$ generated in the fragmentation of CO_2^{3+}. The $P_\parallel$ and $P_\perp$ represent the momentum vectors parallel and perpendicular to the laser polarization axis, respectively. The linearly polarized laser pulses have a central wavelength of 800 nm, a pulse duration of 24 fs, and an intensity of 1×10^{15} W/cm^2. It can be seen that the momentum is directed mainly parallel to the laser polarization for O^+ ions and perpendicular for C^+ ions. The anisotropic angular distributions of the atomic ions originate mainly from dynamic alignment as well as postionization alignment. The former occurs before ionization and the latter occurs after ionization. These two kinds of alignments come from the interaction of the laser electric field and the induced dipole moment of molecules [20]. Fragmentation of CO_2^{3+} into $O^+ + C^+ + O^+$ may take place through the nonsequential fragmentation process (channel 1) or the sequential fragmentation process with an intermediate product CO^{2+} (channel 2):

$$CO_2^{3+} \rightarrow O^+ + C^+ + O^+, \tag{1}$$

$$CO_2^{3+} \rightarrow CO^{2+} + O^+ \rightarrow O^+ + C^+ + O^+. \tag{2}$$

Nonsequential fragmentation of $CO_2{}^{3+}$ in which the two C=O bonds break simultaneously is similar to the nonsequential double ionization of atoms in which the two electrons are stripped away simultaneously. The electron-electron momentum correlation diagram can identify the nonsequential and sequential double ionization of atoms in intense laser fields [21,22]. It is expected that the kinetic energies are comparable for the two O^+ ions in nonsequential fragmentation, just as the momentum vectors of the two electrons in nonsequential double ionization. Therefore, we redraw the experimental data and show the correlation diagram of the kinetic energy of two O^+ ions. The results are shown in Fig. 1(b), which exhibit two obvious regimes separated by a red circle. Outside of the circle, the two O^+ ions have comparable kinetic energies and thus should originate from the nonsequential fragmentation process. Inside the circle, the kinetic energies have no obvious correlation for the two O^+ ions, suggesting their origin from the sequential fragmentation process.

To confirm the energy correlation method of separating sequential and nonsequential fragmentation channels, we draw the Newton plot with the data from these two channels. It is known that the Newton plot can visualize the momentum correlation of reaction products and is effective to identify the fragmentation mechanisms of three-body processes [10]. In the Newton diagram, the momentum vector of the first O^+ ion is represented by an arrow fixed at one arbitrary unit. The momentum vectors of the C^+ ion and the second O^+ ion are normalized to the length of the first O^+ ion momentum vector and mapped in the left of the plot. Figures 2(a) and 2(b), respectively, show the Newton plots of the experimental data from the nonsequential fragmentation and sequential fragmentation of $CO_2{}^{3+}$. In the case of nonsequential fragmentation, we observed a pair of crescent-shaped structures. In the case of sequential fragmentation, we observed a circle structure with the center at -0.5 arbitrary units. The difference of the two structures is caused by the existence of a rotating intermediate CO^{2+} in the sequential fragmentation of $CO_2{}^{3+}$, in which the $CO_2{}^{3+}$ ion first dissociates into an O^+ and an

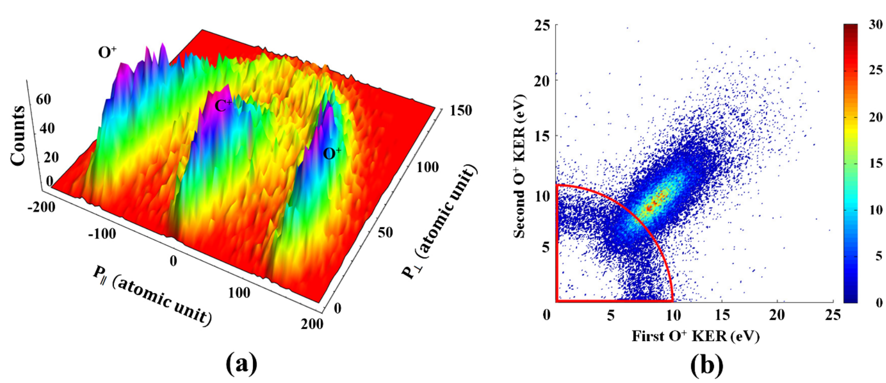

FIG. 1 (color online). (a) Experimentally measured two-dimensional momentum distributions of correlated atomic ions $O^+ + C^+ + O^+$ and (b) kinetic energy release (KER) correlation diagram for two O^+ ions generated in the fragmentation of $CO_2{}^{3+}$ in 800 nm, 24 fs linearly polarized laser fields with an intensity of 1×10^{15} W/cm^2. The data outside the circle come from nonsequential fragmentation and inside the circle from sequential fragmentation.

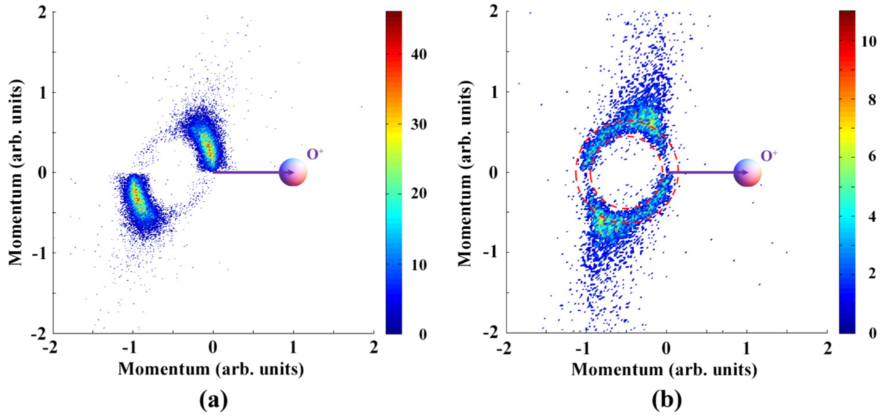

FIG. 2 (color online). Newton plot for three-body fragmentation of ${CO_2}^{3+}$ in intense laser fields. (a) Nonsequential fragmentation and (b) sequential fragmentation. The circle marked by the red dashed line is clear proof of the existence of a rotating intermediate CO^{2+} in the sequential fragmentation.

intermediate CO^{2+}. Some of the dissociation energy will be transformed into the rotational energy of CO^{2+}. Then the CO^{2+} dissociates into a C^+ ion and a second O^+ ion. The accompanying rotation of the intermediate CO^{2+} results in the circle structure in the Newton plot. The consistency between the correlation diagram and the Newton plot shows that both sequential and nonsequential fragmentations occur for ${CO_2}^{3+}$ in intense femtosecond laser fields. According to their counts, the product ratio of the nonsequential to the sequential fragmentation is about 3:1.

The asymptotic angle O^+:O^+ and the kinetic energy releases of correlated $O^+ + C^+ + O^+$ ions are usually used to reconstruct the geometric structure of CO_2^{3+} before fragmentation. Theoretical calculations have shown that the asymptotic angle O^+:O^+ is a little smaller than the initial O-C-O bond angle due to the Coulomb repulsion [15]. Figure 3(a) shows the asymptotic angle O^+:O^+, and the peak value is 135° for sequential fragmentation and 161° for nonsequential fragmentation. The asymptotic angle O^+:O^+ in the nonsequential fragmentation process is much larger than that in the sequential fragmentation process. Thus, the bond angle tends to be underestimated for ${CO_2}^{3+}$ before explosion if the molecular structure is reconstructed without eliminating the data of the sequential fragmentation from the overall fragmentation. As the most probable bond angle is 172.5° for neutral CO_2 molecules before laser irradiation [23], it can also be expected that the change of the bond angle is overestimated for CO_2 molecules after the laser irradiation if the data of sequential fragmentation are not separated from the nonsequential fragmentation.

Figure 3(b) shows the kinetic energy of C^+ generated in nonsequential and sequential fragmentation processes. It is obvious that C^+ kinetic energy has a higher average value and a broader distribution in the sequential fragmentation process than that in the nonsequential fragmentation process. This observation can be explained by the different dissociation patterns between the nonsequential and sequential fragmentation processes. In the sequential fragmentation process, the fragmentation can be divided into two steps due to the existence of a rotating intermediate CO^{2+}. In the first step, the initial ${CO_2}^{3+}$ undergoes dissociation to the first O^+ and CO^{2+}. After a time delay, the second step occurs in which the CO^{2+} further dissociates into a C^+ and the second O^+. The final momentum of the C^+ is the sum of the momentum vectors obtained in these two steps. However, the dissociation of intermediate CO^{2+} is always accompanied by its rotation, as proved by the circle structure in the Newton plot. As a result, there is a broad angle distribution for the momentum vectors of the C^+ ion obtained in the two steps, which lead to the broad distribution of the C^+ kinetic energy. In the case of nonsequential fragmentation, the two C═O bonds break simultaneously. It can be predicted that the C^+ kinetic energy is zero and the two O^+ ions are emitted back-to-back when

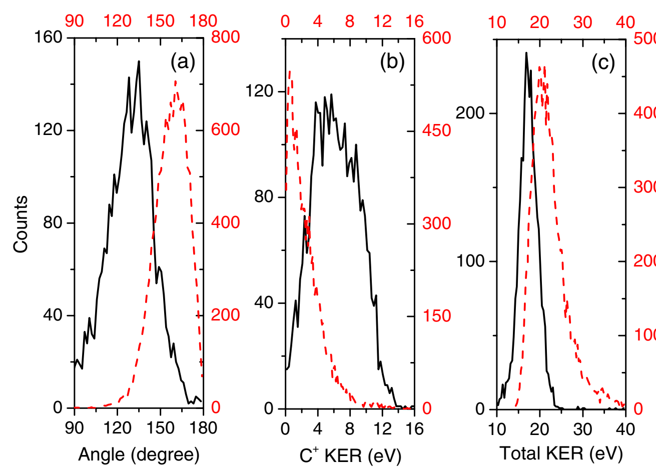

FIG. 3 (color online). (a) Asymptotic angle O^+:O^+ between the momentum vectors of the two O^+ (b) C^+ KER and (c) total KER generated from fragmentation of ${CO_2}^{3+}$ in intense laser fields. Nonsequential fragmentation (red dashed line) and sequential fragmentation (black solid line).

the geometry is linear and symmetric for $CO_2{}^{3+}$, whereas the C^+ would acquire some small kinetic energy when the geometry deviates from linear or becomes unsymmetrical. These predictions are consistent with our observation of a lower average value and narrower distribution for C^+ kinetic energy in the case of nonsequential fragmentation.

Figure 3(c) shows the total kinetic energy releases in the nonsequential and sequential fragmentation processes. The peak is 17.2 eV for sequential fragmentation and 20.7 eV for nonsequential fragmentation. Assuming the nonsequential fragmentation originates from the Coulomb potential, the bond length can be derived to be ~1.7 Å for $CO_2{}^{3+}$ before fragmentation based on the kinetic energy release of 20.7 eV, as shown in Fig. 4. This value agrees with the report given by Hishikawa *et al.*, in which case the CO_2 molecules were irradiated by 100 fs, 795 nm laser pulses at an intensity of 1.1×10^{15} W/cm^2. In comparison with neutral CO_2 molecules, Hishikawa *et al.* thus claimed that there is a large structural deformation for CO_2 subject to intense laser fields [13]. To reveal the origin of the structural deformation of $CO_2{}^{3+}$, Sato *et al.* theoretically investigated the dynamics of structural deformations of CO_2 in an intense femtosecond laser field [24]. They concluded that the structure deformation of $CO_2{}^{3+}$ originates from the structural deformation on laser dressed $CO_2{}^{2+}$. In addition, they predicted that about 100 fs is required for a symmetric bond stretched to 1.75 Å. However, the time of 100 fs is much longer than the pulse duration of ~24 fs in the current experiment. Therefore, the mechanism of symmetric bond stretching on laser dressed $CO_2{}^{2+}$ cannot explain our experimental data. Very recently, Bocharova *et al.* found that the kinetic energy release is always near 21 eV for nonsequential fragmentation of $CO_2{}^{3+}$ with the laser pulse duration varying from 7 to 200 fs [17]. The independence of the kinetic energy release on the pulse duration is intriguing and may indicate that the Coulomb potential is not appropriate to describe the nonsequential

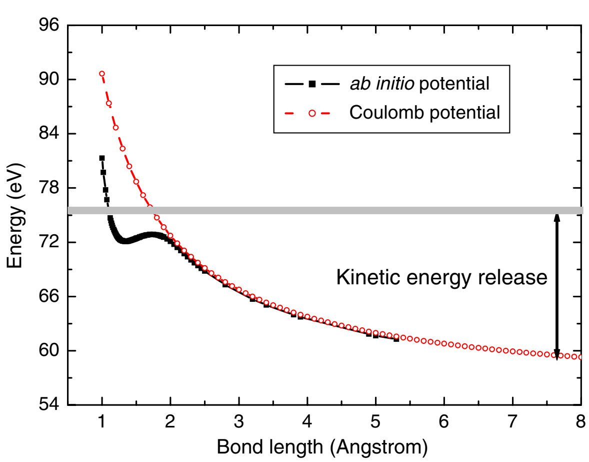

FIG. 4 (color online). Coulomb potential and *ab initio* potential of $CO_2{}^{3+}$.

fragmentation dynamics of $CO_2{}^{3+}$. The predicted large deformation of molecular structure after the laser interaction may originate from the Coulomb potential approximation that has been applied in the reconstruction process of $CO_2{}^{3+}$. As indicated in our previous studies, Coulomb explosion occurs also through non-Coulombic states for lower charged diatomic molecular ions, and the structure change can be overestimated when the Coulomb potential is used to derive the molecular structure [25].

Therefore we calculate the *ab initio* potential energy profile for the dissociation of $CO_2{}^{3+}$ with the CASSCF/CASPT2/aug-cc-pVQZ method using the MOLPRO program package [26]. To describe the nonsequential fragmentation process of $CO_2{}^{3+}$ concisely, the two C=O bond lengths are equally stretched under the linear state of $CO_2{}^{3+}$ in the calculations. Figure 4 shows the calculated results for the field-free lowest adiabatic state of $CO_2{}^{3+}$, in which a saddle point exists around 1.35 Å with a height of 0.77 eV. It can be seen that the Coulomb potential approaches the *ab initio* potential closely when the bond length is larger than 2.1 Å. The agreement of the two potentials at a large bond length verifies the reliability of our theoretical calculations. Using the calculated *ab initio* potential, the C=O bond length is derived to be 1.1 Å, as shown in Fig. 4, which is quite close to the bond length of 1.16 Å for neutral CO_2 molecules [23]. The involvement of a definite electronic state (*ab initio* potential) for the three-body fragmentation of $CO_2{}^{3+}$ can well explain the experimental observation of the independence of the kinetic energy release on the laser pulse duration. These results demonstrate that the application of the Coulomb potential may result in a large discrepancy between the neutral CO_2 molecular structure and the reconstructed molecular structure of $CO_2{}^{3+}$ and thus the overestimation of the structural change after laser irradiation. It shows here that, when imaging the geometry of molecules, *ab initio* potential instead of Coulomb potential is more appropriate for describing the nonsequential fragmentation of molecules upon intense femtosecond laser pulses.

In conclusion, the three-body fragmentation dynamics of $CO_2{}^{3+}$ were experimentally studied in intense laser fields. By using correlation diagrams and Newton plots, we separated and identified nonsequential and sequential fragmentations of $CO_2{}^{3+}$. The geometric structure was therefore accurately reconstructed for $CO_2{}^{3+}$ before fragmentation and turns out to be close to that of the neutral CO_2 molecule before laser irradiation. Our study indicated that Coulomb explosion is a promising approach for imaging geometric structures of polyatomic molecules if the fragmentation dynamics can be clearly clarified for multiply charged molecular ions.

This work was supported by the National Basic Research Program of China (Grants No. 2013CB922403 and No. 2013CB834602), the National Natural Science Foundation of China (Grants No. 61178019, No. 11134001, and No. 11121091), and New Century Excellent Talents from Ministry of Education of China. The calculations were supported by Super-computer Center, CNIC, CAS.

*cywu@pku.edu.cn
†hongmei@iccas.ac.cn
‡qhgong@pku.edu.cn

[1] K. J. Gaffney and H. N. Chapman, Science **316**, 1444 (2007).
[2] A. H. Zewail, Science **328**, 187 (2010).
[3] C. I. Blaga, J. Xu, A. D. Dichiara, E. Sistrunk, K. Zhang, P. Agostini, T. A. Miller, L. F. DiMauro, and C. D. Lin, Nature (London) **483**, 194 (2012).
[4] M. Y. Ivanov, Nature (London) **483**, 161 (2012).
[5] F. Legare, I. V. Litvinyuk, P. W. Dooley, F. Quere, A. D. Bandrauk, D. M. Villeneuve, and P. B. Corkum, Phys. Rev. Lett. **91**, 093002 (2003).
[6] F. Legare, K. F. Lee, I. V. Litvinyuk, P. W. Dooley, A. D. Bandrauk, D. M. Villeneuve, and P. B. Corkum, Phys. Rev. A **72**, 052717 (2005).
[7] E. Gagnon, P. Ranitovic, X. M. Tong, C. L. Cocke, M. M. Murnane, H. C. Kapteyn, and A. S. Sandhu, Science **317**, 1374 (2007).
[8] R. K. Singh, G. S. Lodha, V. Sharma, I. A. Prajapati, K. P. Subramanian, and B. Bapat, Phys. Rev. A **74**, 022708 (2006).
[9] M. R. Jana, P. N. Ghosh, B. Bapat, R. K. Kushawaha, K. Saha, I. A. Prajapati, and C. P. Safvan, Phys. Rev. A **84**, 062715 (2011).
[10] N. Neumann, D. Hant, L. P. H. Schmidt, J. Titze, T. Jahnke, A. Czasch, M. S. Schoffler, K. Kreidi, O. Jagutzki, H. Schmidt-Bocking, and R. Dorner, Phys. Rev. Lett. **104**, 103201 (2010).
[11] L. J. Frasinski, P. A. Hatherly, K. Codling, M. Larson, A. Persson, and C. G. Wahlstrom, J. Phys. B **27**, L109 (1994).
[12] C. Cornaggia, Phys. Rev. A **54**, R2 555 (1996).
[13] A. Hishikawa, A. Iwamae, and K. Yamanouchi, Phys. Rev. Lett. **83**, 1127 (1999).
[14] W. A. Bryan, J. H. Sanderson, A. El-Zein, W. R. Newell, P. F. Taday, and A. J. Langley, J. Phys. B **33**, 745 (2000).
[15] K. Zhao, G. Zhang, and W. T. Hill, III, Phys. Rev. A **68**, 063408 (2003).
[16] J. P. Brichta, S. J. Walker, R. Helsten, and J. H. Sanderson, J. Phys. B **40**, 117 (2007).
[17] I. Bocharova *et al.*, Phys. Rev. Lett. **107**, 063201 (2011).
[18] Y. Liu, X. Liu, Y. Deng, C. Wu, H. Jiang, and Q. Gong, Phys. Rev. Lett. **106**, 073004 (2011).
[19] C. Y. Wu, Y. D. Yang, Y. Q. Liu, Q. H. Gong, M. Wu, X. Liu, X. L. Hao, W. D. Li, X. T. He, and J. Chen, Phys. Rev. Lett. **109**, 043001 (2012).
[20] X. M. Tong, Z. X. Zhao, A. S. Alnaser, S. Voss, C. L. Cocke, and C. D. Lin, J. Phys. B **38**, 333 (2005).
[21] M. Lein, E. K. U. Gross, and V. Engel, Phys. Rev. Lett. **85**, 4707 (2000).
[22] W. Becker, X. Liu, P. J. Ho, and J. H. Eberly, Rev. Mod. Phys. **84**, 1011 (2012).
[23] B. Siegmann, U. Werner, H. O. Lutz, and R. Mann, J. Phys. B **35**, 3755 (2002).
[24] Y. Sato, H. Kono, S. Koseki, and Y. Fujimura, J. Am. Chem. Soc. **125**, 8019 (2003).
[25] C. Wu, Y. Yang, Z. Wu, B. Chen, H. Dong, X. Liu, Y. Deng, H. Liu, Y. Liu, and Q. Gong, Phys. Chem. Chem. Phys. **13**, 18 398 (2011).
[26] MOLPRO, version 2009.1, a package of *ab initio* programs: H. J. Werner, P. J. Knowles, R. Lindh, F. R. Manby, and M. Schütz; see http://www.molpro.net. All the potential energies were calculated by the CASSCF method first and then improved by the CASSCF second-order perturbation theory (CASPT2) method. The selected active space comprises 13 electrons and 12 orbitals. The full valence active space is named (32203110), upon labeling these active orbitals within the D_{2h} subgroup of $D_{\infty h}$ in the order of A_g, B_{3u}, B_{2u}, B_{1g}, B_{1u}, B_{2g}, B_{3g}, and A_u.